

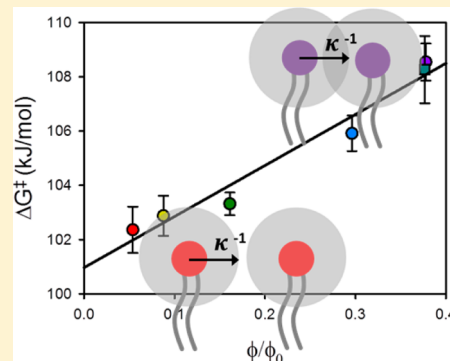
# Phosphatidylglycerol Flip-Flop Suppression due to Headgroup Charge Repulsion

Krystal L. Brown and John C. Conboy\*

Department of Chemistry, University of Utah, 315 South 1400 East, RM 2020, Salt Lake City, Utah 84103, United States

## S Supporting Information

**ABSTRACT:** The kinetics and thermodynamics of 1,2-distearoyl-*sn*-glycero-3-[phospho(1'-*rac*-glycerol)] (DSPG) flip-flop in 1,2-distearoyl-*sn*-glycero-3-phosphocholine (DSPC) membranes were examined by sum-frequency vibrational spectroscopy (SFVS). The effect of DSPG concentration in the membrane and the influence of electrolyte concentration were examined in an attempt to decipher the role the anionic PG headgroup plays in dictating the dynamics of PG flip-flop for this biologically important lipid species. DSPG flip-flop dynamics and the activation barrier to exchange were found to be directly dependent on the amount of DSPG present in the bilayer. Analysis of the activation free energy for DSPG flip-flop in mixed DSPG + DSPC bilayers reveals that charge repulsion between neighboring PG headgroups modulates the free energy barrier and subsequently, the rate of translocation. Specifically, when DSPG comprises a small portion of the bilayer, the electrostatic potential of neighboring PG lipids are effectively shielded from each other under high ionic strength conditions and little to no charge repulsion occurs. When DSPG lipids are close enough to experience charge repulsion from neighboring PG lipids, as in bilayers containing a large fraction of DSPG, or for bilayers in low ionic strength solutions, the influence of charge repulsion on the energetics of lipid flip-flop are measurable. For biological membranes, where the concentration of PG is relatively low, the neighboring PG lipids are spaced far enough apart that their anionic charges are effectively shielded, such that under physiological conditions the charged nature of the headgroup does little to modulate its lipid flip-flop energetics and corresponding rate of translocation.



## INTRODUCTION

Cellular membranes contain a varied library of lipids that allow each membrane to be tailored for its specific functions.<sup>1</sup> For example, phospholipids in plant, animal, and bacterial cells possess five main headgroup chemistries: phosphatidylcholine (PC), phosphatidylethanolamine (PE), phosphatidylserine (PS), phosphatidylinositol (PI), and phosphatidylglycerol (PG).<sup>1,2</sup> The complexity and nuances of membrane lipid diversity have made the specific biological function of this headgroup diversity an active area of research. For example, the anionic lipids PS, PI, and PG are of particular importance due to the multitude of cellular responses associated with these lipid species.<sup>1,3–5</sup>

While PS and PI are the major anionic lipids of eukaryotic membranes, PG is mainly found in prokaryotic membranes with<sup>1,3,4</sup> the biological concentrations of PG lipids varying widely between organisms and even within different membranes of the same organism.<sup>1,4</sup> Although its presence in the plasma membrane of mammalian cells is limited, PG comprises about 10% of the phospholipid content of eukaryotic mitochondria,<sup>6,7</sup> is a major constituent of bacterial membranes, and is found in plant membranes especially in the chloroplasts.<sup>8</sup> PG lipids are also unique in that their headgroup chemistry results in a high degree of solvation and hydrogen-bonding capacity.<sup>4,9</sup>

Key to the functioning of anionic lipid species, such as PG, is their ability to traverse the membrane in response to both external and internal stimuli. The exchange of lipids between membrane leaflets, known as lipid flip-flop, has been shown to be particularly sensitive to headgroup polarity, size, and charge using a variety of probe based methods employing fluorescence, ESR, and NMR spectroscopies.<sup>3,10–24</sup> The asymmetric distribution of anionic lipids resulting from lipid flip-flop is known to play an active role in cellular function, ranging from the modulation of cell signaling events to affecting membrane shape and stiffness.<sup>4,5,25,26</sup> Studies on PG transbilayer movement have been performed using fluorescent lipid probes;<sup>17</sup> however, there is no information available on native (unlabeled), protein-free, PG flip-flop dynamics. We have previously shown that chemical modification of lipids results in altered flip-flop dynamics,<sup>27</sup> underscoring the need for label-free methods for measuring native lipid translocation. The past decade has seen an emergence of techniques capable of making such measurements in model membranes, including small angle neutron scattering,<sup>28</sup> shape changes in large unilamellar vesicles,<sup>29</sup> AFM,<sup>30</sup> and sum-frequency vibrational spectroscopy (SFVS).<sup>27,31–42</sup>

Received: June 9, 2015

Revised: July 14, 2015

SFVS is a spectroscopic method which does not require labeling of the lipids with a fluorescent or other probe to measure lipid translocation and is capable of isolating the energetic impact of specific lipid properties, such as headgroup chemistry, acyl chain length, and membrane composition on native lipid translocation.<sup>27,31–35,37–39</sup>

As discussed in detail in our previous publications, SFVS can be used to readily determine the population difference of proteated versus deuterated lipids between the leaflets of planar supported lipid bilayers, allowing for the precise determination of lipid asymmetry and flip-flop dynamics in a nonperturbing fashion. In particular, our previous SFVS studies have shown that the methyl symmetric stretch ( $\text{CH}_3 \nu_s$ ) is inherently sensitive to the lipid population difference in a bilayer providing a simple relationship between the measured  $\text{CH}_3 \nu_s$  intensity and the population difference of deuterated to proteated lipids in a membrane:

$$I_{\text{CH}_3} \propto (N_B - N_T)^2 \quad (1)$$

where  $N_B$  and  $N_T$  are the fraction of proteated lipids in the bottom (B) and top (T) leaflets of a bilayer, respectively.<sup>27,39</sup>

This relationship is also used to relate the measured time-dependent SFVS intensity to the rate of lipid flip-flop using the following equation:

$$I_{\text{CH}_3}(t) = I_{\text{R,max}} e^{-4kt} + I_{\text{R,min}} \quad (2)$$

where  $I_{\text{R,max}}$  and  $I_{\text{R,min}}$  are the resonant SFVS responses when  $N_B - N_T = 1$  and 0, respectively.<sup>27,39</sup> Nonzero values for  $I_{\text{R,min}}$  are possible due to background scattering from the visible beam and electronic offsets in the measurement system.

The kinetic information derived from the SFVS experiments is essential for determining the time scale of lipid translocation. The kinetic data provide a means to readily assess the Gibbs activation thermodynamics for lipid flip-flop using transition-state theory (TST). The transition-state free energy ( $\Delta G^\ddagger$ ) is a convenient means to quantify the barrier height for lipid flip-flop as this determines the kinetics or rate of lipid translocation in bilayer systems. TST also provides a convenient means of uncovering the enthalpic and entropic contributions to lipid exchange, and the underlying chemical and physical directors of lipid translocation. This information provides the framework for understanding the energetic barrier protein mediated flip-flop must overcome in order to catalyze this process in living cells. We have previously utilized SFVS to quantify the kinetics and thermodynamics of lipid flip-flop for a number of systems: single component PC bilayers,<sup>27,39</sup> the flip-flop of PE and PS lipids,<sup>33,37</sup> the effect of membrane packing on lipid flip-flop,<sup>32,34</sup> and the influence of cholesterol and transmembrane peptides on lipid translocation.<sup>31,35,38</sup>

In the present study, SFVS is used to quantify the kinetics and thermodynamics of lipid flip-flop in bilayers composed of 1,2-distearoyl-*sn*-glycero-3-[phospho(1'-*rac*-glycerol)] (DSPG) and 1,2-distearoyl-*sn*-glycero-3-phosphocholine (DSPC) (Figure 1). The effect of DSPG concentration in the membrane and the influence of electrolyte concentration were examined in an attempt to decipher the role the anionic PG headgroup plays in dictating the dynamics of PG flip-flop for this biologically important lipid species.

## MATERIALS AND METHODS

**Materials.** DSPG, DSPC, and their deuterated counterparts, 1,2-distearoyl-*d*70-*sn*-glycero-3-[phospho-*rac*-(1-glycerol)]

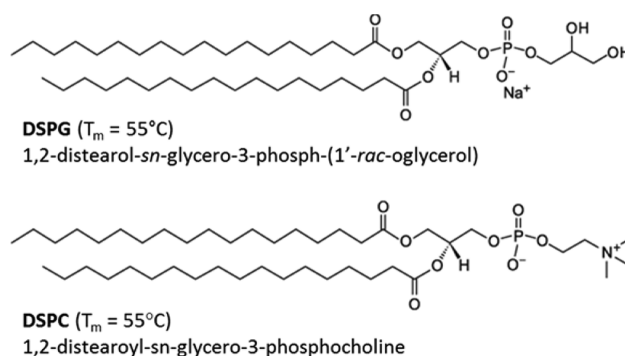


Figure 1. Chemical structures for DSPG and DSPC.

(DSPGd70) and 1,2-distearoyl-*d*70-*sn*-glycero-3-phosphocholine (DSPCd70), were obtained from Avanti Polar Lipids (Alabaster, AL, USA) and used without further purification. GC grade chloroform and methanol were obtained from Mallinckrodt (Phillipsburg, NJ, USA) and used as received. Nanopure water (Barnstead Thermolyne, Dubuque, IA, USA) was used with a minimum resistivity of 18.2  $\text{M}\Omega\cdot\text{cm}$ . Deuterium oxide was obtained from Sigma-Aldrich (St. Louis, MO, USA) and purified with a 2  $\mu\text{m}$  filter before use. High ionic strength phosphate buffered saline (PBS) was prepared from 10 mM  $\text{Na}_2\text{HPO}_4$ , 2 mM  $\text{NaH}_2\text{PO}_4$ , and 137 mM NaCl in water and adjusted to a pH of 7.2 using dilute HCl. Low ionic strength PBS was prepared from 3 mM  $\text{Na}_2\text{HPO}_4$ , 0.6 mM  $\text{NaH}_2\text{PO}_4$ , and 39 mM NaCl in water and adjusted to a pH of 7.2 using dilute HCl. UV-grade fused silica prisms were obtained from Almaz Optics (Marlton, NJ, USA) and used as planar supports for the lipid bilayers in this study. The prisms were cleaned in a UV-ozone cleaner (Jelight Co., Irvine, CA, USA) for 15 min. After rinsing thoroughly with water, the prism was immersed in a solution of 70% 18 M sulfuric acid and 30%  $\text{H}_2\text{O}_2$  for a minimum of 30 min. (**CAUTION! This solution is a strong oxidant and reacts violently with organic solvents. Extreme caution must be taken when handling the solution.**) The prisms were rinsed thoroughly with water, dried in  $\text{N}_2$  gas, and cleaned with Ar plasma (Harrick Scientific, Ithaca, NY, USA) for 2–4 min prior to bilayer preparation.

**Bilayer Preparation.** Lipid solutions were prepared at a concentration of 1 mg/mL in a 65:35:8 mixture of  $\text{CHCl}_3$ :MeOH: $\text{H}_2\text{O}$  by volume. Binary lipid mixtures with 10, 14.3, 25, 50, and 75 mol % DSPG in DSPC were prepared by combining the appropriate quantities of single lipid solutions to achieve the desired ratios. These mixtures were prepared such that only one lipid species in each bilayer would give rise to a SFVS signal. One bilayer leaflet was composed of a mixture of DSPGd70 and DSPCd70, which does not give rise to any SFVS signal in the spectral region being investigated here. The second leaflet contained the same percentage of either DSPG and DSPCd70 or DSPGd70 and DSPC, to monitor only the proteated DSPG or DSPC component, respectively.

All lipid bilayers were prepared using a PBS subphase by the Langmuir–Blodgett/Langmuir–Schaefer method. This method has been described in detail elsewhere.<sup>43</sup> Briefly, a lipid solution was spread at the air/water interface of a KSV Instruments minitrough (Helsinki, Finland). The lipid solution was allowed to equilibrate for 15–30 min before being compressed to a surface pressure of 30 mN/m at 25  $^\circ\text{C}$ . The prism was vertically withdrawn through the subphase at a speed of 3 mm/min to deposit the first (or proximal) leaflet. The top (or distal) leaflet

was deposited by spreading a new lipid solution at the air/water interface, compressing to 30 mN/m at 25 °C, and horizontally submerging the prism through the subphase. The bilayer was maintained in an aqueous environment after preparation and assembly in a custom built Teflon flow cell. The flow cell was rinsed with PBS prepared in D<sub>2</sub>O in order to avoid spectral overlap with water.

**Pressure–Area Isotherms.** Pressure–area isotherms were performed on the LB trough to measure the mean molecular area of the DSPG + DSPC membranes. A lipid monolayer was initially deposited at the air/water interface of the Langmuir trough at a low surface pressure (<1 mN/m) and compressed to collapse pressure (~45 mN/m). The surface pressure of the film was recorded as a function of the mean molecular area of the lipids to determine the packing density at 30 mN/m at 25 °C.

**SFVS Measurements.** The SFVS setup used for these experiments is described in detail elsewhere.<sup>27,39</sup> Briefly, an OPO/OPA system (LaserVision, Bellevue, WA, USA) was pumped by the fundamental 1064 nm output of a 10 Hz Nd:YAG laser (Continuum, Santa Clara, CA, USA) to produce a fixed visible beam at 532 nm and a tunable mid-IR beam. The bandwidths of the 532 nm and IR were 1 and 3 cm<sup>-2</sup>, respectively. The visible beam was collimated to about 5 mm<sup>2</sup> with a power of about 7 mJ/pulse. The IR beam was about 6 mm<sup>2</sup> with a power of about 3 mJ/pulse. The visible and IR beams were directed at the prism surface at angles of 67° and 62°, respectively, and the resulting sum-frequency beam was collected by a PMT (Hamamatsu Photonics, Hamamatsu, Japan) and integrated by a boxcar integrator (Stanford Research Systems, Sunnyvale, CA, USA).

SFVS spectra were obtained by scanning the input IR beam from 2700 to 3100 cm<sup>-1</sup> in 2 cm<sup>-1</sup> steps and integrating for 3 s at each step. SFVS decays were collected by monitoring the SFVS signal at the CH<sub>3</sub>  $\nu_s$  frequency of 2875 cm<sup>-1</sup> as a function of time. Bilayers were heated to the desired temperature using a circulating water bath (HAAKE Phoenix II P1 Circulator, Thermo Fisher Scientific). The temperature in the flow cell was monitored with a type K thermocouple. The time-dependent SFVS signal was integrated in intervals of at least 3 s, truncated to remove the data prior to temperature stabilization (about 15 min), and fit to eq 2 to determine the rate of lipid flip-flop. All lipid flip-flop kinetics were collected at a temperature below the phase transition temperature ( $T_m$ ) of DSPG and DSPC at 55 °C, as the rates of lipid translocation are too rapid to measure near or above the  $T_m$ . The lower temperature limit of the kinetic data was determined by a reasonable acquisition time over which environmental variables could be held relatively constant, which was around 10 h.

## RESULTS AND DISCUSSION

### SFVS Spectra of DSPG + DSPC Lipid Bilayers.

Representative SFVS spectra for mixed DSPG + DSPC bilayers recorded in high ionic strength PBS (~150 mM) are shown in Figure 2a. These spectra correspond to bilayers composed of 10%, 14.3%, 25%, 50%, and 75% DSPG in DSPCd70, with only the DSPG component giving rise to the measured SFVS response. All five spectra show a peak at 2875 cm<sup>-1</sup> from the CH<sub>3</sub>  $\nu_s$  of the terminal methyl group of the acyl chains. The CH<sub>2</sub>  $\nu_s$  is observed as a shoulder at 2850 cm<sup>-1</sup>. The peak at 2940 cm<sup>-1</sup> is a combination of the CH<sub>3</sub> Fermi resonance at 2905 cm<sup>-1</sup> and the CH<sub>2</sub> asymmetric stretch at 2960 cm<sup>-1</sup>. The spectra of DSPG are consistent with those previously obtained

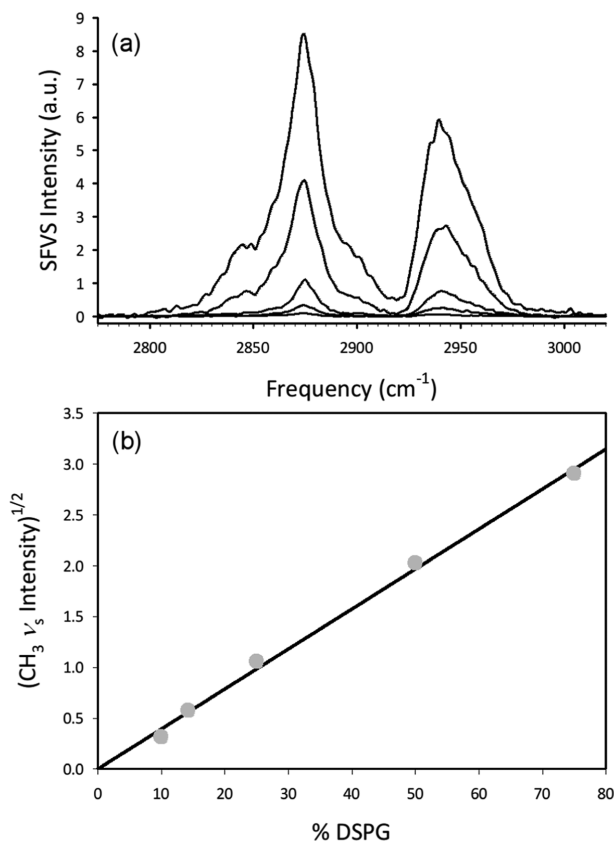


**Figure 2.** (a) Representative spectra of lipid bilayers composed of 10%, 14.3%, 25%, 50%, and 75% DSPG which have been normalized for comparison and appear in descending order. Only the proteated DSPG lipid component gives rise to the measured SFVS signal. (b) Square root of the CH<sub>3</sub>  $\nu_s$  intensity shown in part a as a function of the percent of DSPG.

for DSPC, DSPE, and DSPS and served as the basis for the spectral assignments given previously.<sup>27,33,37</sup> The spectra shown in Figure 2a quantitatively demonstrate the relationship between the measured SFVS intensity and the number of proteated lipids in the bilayer (eq 1). All vibrational signatures in the spectra are unchanged, but decrease in intensity as the fraction of proteated DSPG decreases. A plot of the square root of the CH<sub>3</sub>  $\nu_s$  peak intensity at 2875 cm<sup>-1</sup> as a function of bilayer composition is shown in Figure 2b, with the linear regression to the data revealing the quantitative linear correlation described in eq 1 with regard to the fraction of proteated DSPG in the membranes.

**Kinetics of Lipid Flip-Flop in DSPG + DSPC Bilayers.** As described earlier, the CH<sub>3</sub>  $\nu_s$  is directly related to the population difference of proteated lipids in the bilayer. By recording the CH<sub>3</sub>  $\nu_s$  intensity as a function of time and temperature, the flip-flop of DSPG can be followed in real time. Representative decay curves for the DSPG component of the mixed DSPG + DSPC bilayers as a function of DSPG composition obtained in high ionic strength PBS are shown in Figure 3. All decay curves in Figure 3 have been normalized for comparison at time  $t = 0$  which was set at the point when the system reached thermal equilibrium.

The decay curves were fit to eq 2, and the measured rates of DSPG flip-flop are summarized in Table 1. The half-life for lipid flip-flop was calculated using



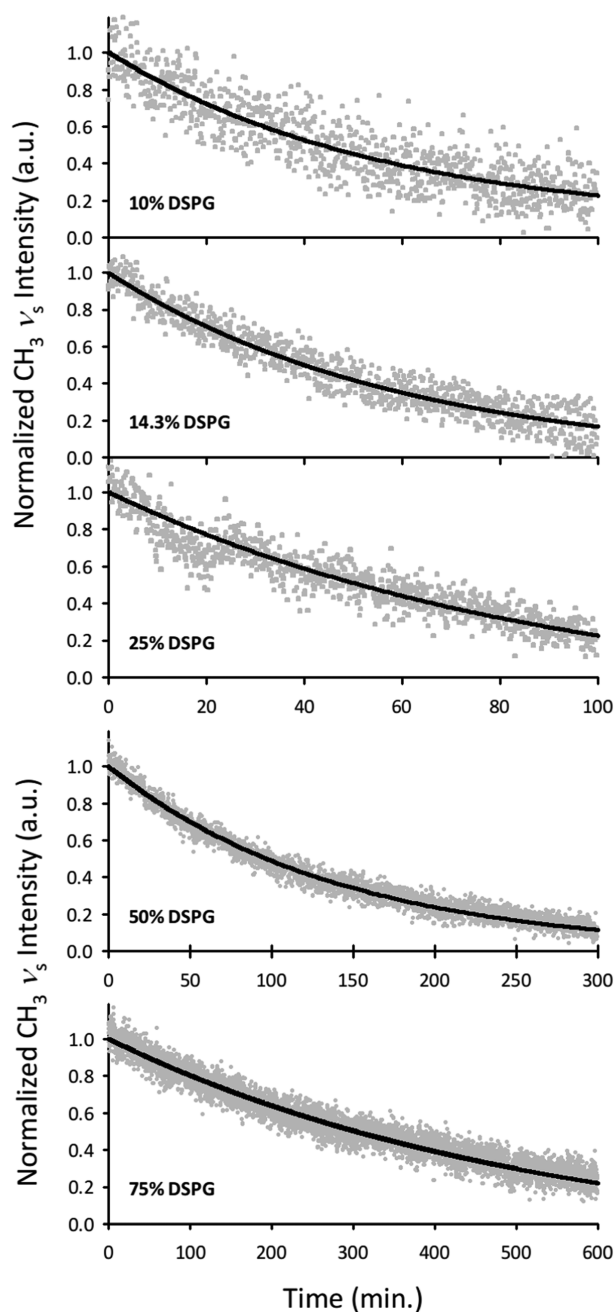


**Figure 3.** Representative DSPG flip-flop kinetics in lipid bilayers composed of 10%, 14.3%, 25%, 50% and 75% DSPG recorded at approximately 44 °C. The solid line represents the fit to the data using eq 2.

$$t_{1/2} = \frac{\ln(2)}{2k} \quad (3)$$

where  $k$  is the rate derived from the experimental data using eq 2. These values are included in Table 1 for comparison.

The rates of DSPG flip-flop are very similar in bilayers containing small amounts of DSPG. This is clearly demonstrated by comparing the half-life for lipid flip-flop at approximately 44 °C in bilayers composed of 10%, 14.3%, and 25% DSPG, which are  $84 \pm 9$ ,  $79 \pm 4$ , and  $99 \pm 5$  min, respectively. The similar kinetics for this wide range of DSPG compositions is somewhat surprising given that DSPG increases by 15 mol % across the series.

**Table 1. Kinetics of DSPG Flip-Flop**

bilayer composition	$T$ (°C)	$k$ ( $\times 10^5$ s $^{-1}$ )	$t_{1/2}$ (min)
10% DSPG	$36.73 \pm 0.06$	$1.18 \pm 0.04$	$489 \pm 16$
	$38.1 \pm 0.2$	$1.87 \pm 0.04$	$309 \pm 7$
	$40.96 \pm 0.09$	$4.4 \pm 0.8$	$132 \pm 23$
	$43.5 \pm 0.2$	$6.9 \pm 0.8$	$84 \pm 9$
14.3% DSPG	$38.29 \pm 0.08$	$1.45 \pm 0.02$	$400 \pm 6$
	$39.3 \pm 0.2$	$2.08 \pm 0.05$	$278 \pm 7$
	$39.7 \pm 0.4$	$2.29 \pm 0.5$	$252 \pm 53$
	$44.42 \pm 0.09$	$7.3 \pm 0.4$	$79 \pm 4$
25% DSPG	$43.0 \pm 0.2$	$3.9 \pm 0.1$	$149 \pm 5$
	$43.96 \pm 0.06$	$5.8 \pm 0.3$	$99 \pm 5$
	$44.5 \pm 0.6$	$6.48 \pm 0.08$	$89 \pm 1$
	$50.1 \pm 0.2$	$25.3 \pm 0.6$	$22.9 \pm 0.5$
50% DSPG	$45.2 \pm 0.2$	$2.99 \pm 0.02$	$193 \pm 1$
	$47.4 \pm 0.2$	$5.11 \pm 0.02$	$113.0 \pm 0.5$
	$49.8 \pm 0.1$	$9.86 \pm 0.09$	$58.6 \pm 0.5$
	$51.1 \pm 0.2$	$15.3 \pm 0.6$	$38 \pm 2$
75% DSPG	$42.76 \pm 0.09$	$0.61 \pm 0.01$	$955 \pm 22$
	$45.8 \pm 0.1$	$1.041 \pm 0.009$	$555 \pm 5$
	$47.9 \pm 0.2$	$2.09 \pm 0.01$	$276 \pm 2$
	$50.08 \pm 0.07$	$4.38 \pm 0.06$	$132 \pm 2$
	$52.26 \pm 0.07$	$7.8 \pm 0.1$	$74 \pm 1$

In order to more fully probe the impact of the PG headgroup on flip-flop kinetics, bilayers containing much higher fractions of DSPG were also investigated. For bilayers composed of 50% DSPG, a marked change in DSPG kinetics is observed, with a half-life of  $193 \pm 1$  min at 45 °C. This half-life is nearly double that for bilayers composed of 25% DSPG at a similar temperature. A significant decrease in the measured rate of DSPG translocation is also observed in bilayers composed of 75% DSPG, which had a measured half-life of  $555 \pm 5$  min near 45 °C. The measured kinetics for DSPG in these mixed bilayers suggests that the quantity of the PG lipids in a membrane plays a direct role on the rate of DSPG flip-flop. A more complete understanding of the factors responsible for modulating the rate of DSPG translocation can be uncovered by examining the activation thermodynamics of PG flip-flop.

**Activation Energy of DSPG Flip-Flop.** The activation free energy,  $\Delta G^\ddagger$ , of DSPG flip-flop was calculated from the measured rates ( $k$ ) using TST:

$$\Delta G^\ddagger = -RT \ln \left( k \frac{h}{k_B T} \right) \quad (4)$$

where  $\Delta G^\ddagger$  is the free energy of activation,  $k_B$  is Boltzman's constant,  $h$  is Planck's constant,  $T$  is the temperature in Kelvin, and  $R$  is the gas constant.<sup>44,45</sup> Figure 4 is a plot of the activation free energy as a function of temperature for each DSPG concentration. A linear regression of the data in Figure 4 was performed using Gibb's equation:

$$\Delta G^\ddagger = \Delta H^\ddagger - T \Delta S^\ddagger \quad (5)$$

where  $\Delta H^\ddagger$  and  $\Delta S^\ddagger$  are the activation enthalpy and activation entropy, respectively. The activation free energy as a function of temperature for pure DSPC flip-flop is also included in Figure 4<sup>34,39</sup> to provide a baseline for the energetic impact of the PG headgroup on lipid translocation.

Examination of the data in Figure 4 reveals that the  $\Delta G^\ddagger$  for DSPG flip-flop decreases slightly in bilayers composed of 10% DSPG relative to bilayers of only DSPC. When the amount of

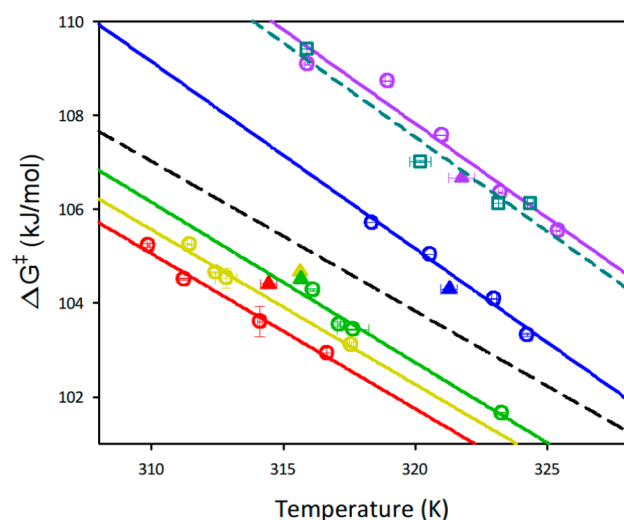


**Figure 4.** Temperature dependence of the activation energy of DSPG flip-flop as a function of bilayer composition [10% (red), 14.3% (yellow), 25% (green), 50% (blue), and 75% (purple)] measured in high ionic strength PBS. The linear regressions shown are the fits to the data using eq 5. The calculated activation energies for DSPC (black line) in this temperature range have been extrapolated from the data in refs 34 and 39. The triangles represent the  $\Delta G^\ddagger$ s for the DSPC component as a function of DSPG concentration. The squares represent the energetics of DSPG flip-flop for a 25% DSPG bilayer in low ionic strength buffer.

DSPG is increased to 14.3% and 25% DSPG, the activation energies increase slightly. Although these bilayer compositions approximate biological ratios of PG and PC lipids, the minor changes observed in  $\Delta G^\ddagger$  make it difficult to draw conclusions regarding the energetic impact of the PG headgroup from these data alone. The  $\Delta G^\ddagger$ s for flip-flop in bilayers composed of 50% DSPG are higher than the  $\Delta G^\ddagger$ s for pure DSPC. This reflects the significant decrease in the rate of flip-flop in this bilayer composition. This trend continues in bilayers composed of 75% DSPG:DSPC, which again show a significant increase in  $\Delta G^\ddagger$  for lipid flip-flop relative to the other bilayer compositions investigated.

The kinetics and activation energies presented thus far have represented only the DSPG component of the bilayers. The DSPC component of these bilayers was also examined by switching the deuterated and proteated lipid species to DSPGd70 and DSPC, respectively, for each bilayer composition. The  $\Delta G^\ddagger$  for DSPC flip-flop has been included in Figure 4, and the activation free energies lie on or near the measured values obtained for DSPG flip-flop. This indicates that the energetics for lipid flip-flop are identical for both lipid components in the mixed DSPG + DSPC bilayers examined here. This finding is consistent with our previous SFVS studies of the kinetics of lipid flip-flop in mixed DSPC + DSPE bilayers where the lipid components differed only in headgroup chemistry and were completely miscible.<sup>33</sup> As such, the energetic trends reported here for DSPG flip-flop are representative of both the DSPG and DSPC components in these bilayers.

In order to directly compare the activation energies for DSPG flip-flop, the linear regressions in Figure 4 were used to extrapolate the  $\Delta G^\ddagger$  at a fixed temperature, 40 °C, for all bilayer compositions. These data are summarized in Table 2 and plotted as a function of bilayer composition in Figure 5a. The  $\Delta G^\ddagger$  for DSPC flip-flop was determined at 40 °C from our

**Table 2. Transition-State Thermodynamics for DSPG and DSPC Flip-Flop**

DSPG (%)	$\Delta G^\ddagger$ (kJ/mol) <sup>a</sup>	$\Delta H^\ddagger$ (kJ/mol)	$\Delta S^\ddagger$ (J/(mol·K))	$T\Delta S^\ddagger$ (kJ/mol) <sup>a</sup>
High Ionic Strength				
10	102.4 ± 0.9	207 ± 9	330 ± 30	105 ± 10
14.3	102.9 ± 0.7	208 ± 10	329 ± 33	105 ± 11
25%	103.3 ± 0.4	212 ± 12	341 ± 38	109 ± 12
50	105.9 ± 0.7	233 ± 12	398 ± 36	127 ± 12
75	108.5 ± 0.7	236 ± 17	400 ± 52	127 ± 16
Low Ionic Strength				
25	108 ± 1	236 ± 22	401 ± 68	128 ± 22
DSPC <sup>b</sup>				
	104.4 ± 0.7	206 ± 26	319 ± 81	101 ± 26

<sup>a</sup>Values are for 40 °C. <sup>b</sup>Values extrapolated from the data given in refs 34 and 39.

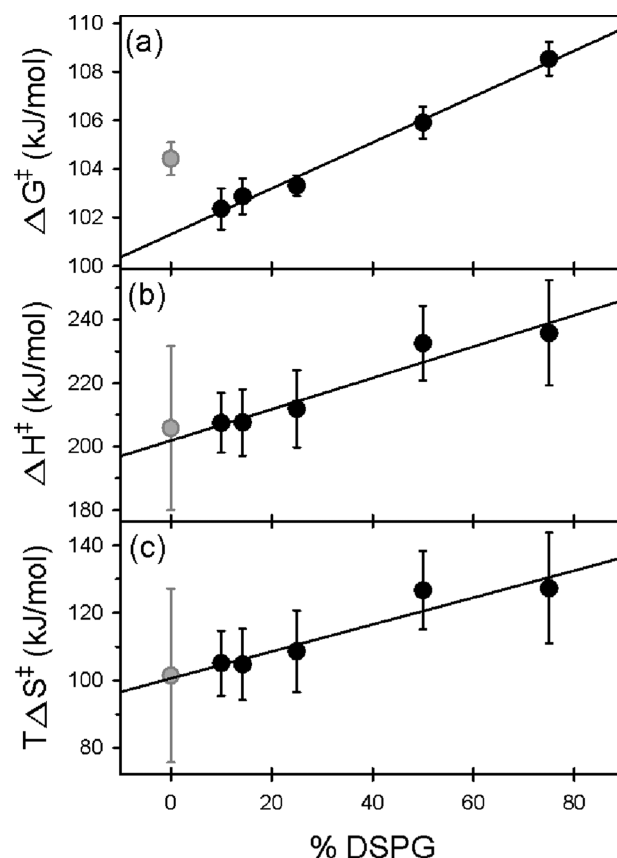


**Figure 5.** (a)  $\Delta G^\ddagger$ , (b)  $\Delta H^\ddagger$ , and (c)  $T\Delta S^\ddagger$  for DSPG flip-flop at 40 °C plotted as a function of bilayer composition. The activation thermodynamics for a single component bilayer composed of DSPC (gray) have been included but were not used in the determination of the linear regression shown for DSPG and are present for comparison purposes.

previous studies<sup>27,34</sup> and included as a reference point. The reported error for the activation energies was determined from the errors obtained in the regression analysis.

The  $\Delta G^\ddagger$  for DSPG flip-flop in bilayers composed of 10% DSPG:DSPC (102.4 ± 0.9 kJ/mol) is slightly lower than that of DSPC (104.4 ± 0.7 kJ/mol). As the amount of DSPG is increased from 14.3% to 25% DSPG:DSPC, the  $\Delta G^\ddagger$  increases slightly to 102.9 ± 0.7 and 103.8 ± 0.4 kJ/mol, respectively. This represents no statistically relevant change in  $\Delta G^\ddagger$  despite a

significant change in the amount of PG in these bilayers. However,  $\Delta G^\ddagger$ s for flip-flop in bilayers composed of 50% and 75% DSPG:DSPC bilayers increase to  $105.9 \pm 0.7$  and  $108.5 \pm 0.7$  kJ/mol, respectively. The measured activation energies for DSPG flip-flop are also in the range of values determined from molecular dynamics simulations ( $105 \pm 6$  kJ/mol),<sup>46</sup> which are associated with the energetic penalty of translocating the hydrophilic headgroup through the hydrophobic membrane core, the conformational disorder induced in the lipid tails, and the changes in headgroup solvation and solvent structure.

Figure 5a shows that there is an overall linear trend of increasing  $\Delta G^\ddagger$  with increasing PG, despite the small apparent changes in the  $\Delta G^\ddagger$  at low concentrations. Figure 5a also reveals that the  $\Delta G^\ddagger$  for lipid flip-flop in bilayers containing small amounts of DSPG (<25 mol %) is lower than that of DSPC flip-flop. The physical underpinnings responsible for these energetics were investigated by determining the activation enthalpies and entropies for DSPG flip-flop from the data in Figure 4.

#### Activation Enthalpy and Entropy for DSPG Flip-Flop.

The activation enthalpy,  $\Delta H^\ddagger$ , is the main component of the energy barrier to lipid flip-flop due to the loss of favorable enthalpic interactions, such as headgroup–water hydrogen bonds.<sup>34</sup> The  $\Delta H^\ddagger$  for DSPG flip-flop was determined from the intercept of the fits in Figure 4. These data are summarized in Table 2 along with the value for pure DSPC.  $\Delta H^\ddagger$ s for DSPG flip-flop in bilayers composed of 10%, 14.3%, and 25% DSPG:DSPC are  $207 \pm 9$ ,  $208 \pm 10$ , and  $212 \pm 12$  kJ/mol, respectively. These values are statistically identical to the  $\Delta H^\ddagger$  for DSPC flip-flop ( $206 \pm 26$  kJ/mol). As observed with the  $\Delta G^\ddagger$ s, very little is revealed by the activation enthalpies of these bilayers containing low amounts of DSPG. Given the strong hydrogen bonds PG headgroups form with surrounding water,<sup>4,9</sup> it is surprising that the activation enthalpies are not more affected, even at low concentrations of DSPG. In comparison,  $\Delta H^\ddagger$  increase to  $233 \pm 12$  and  $236 \pm 17$  kJ/mol for DSPG flip-flop in bilayers composed of 50% and 75% DSPG:DSPC, respectively. This represents a significant increase in the enthalpic barrier to lipid flip-flop at these higher fractions of DSPG. Examination of the activation enthalpies for the complete range of DSPG reveals an overall linear trend of increasing  $\Delta H^\ddagger$  with increasing PG.

The activation entropy,  $\Delta S^\ddagger$ , for DSPG flip-flop in these DSPG + DSPC bilayers was determined from the slope of the fit to eq 5 (Figure 4) and reported in Table 2. The total contribution to the activation barrier,  $T\Delta S^\ddagger$  at 40 °C is also included, along with the values for pure DSPC flip-flop. The  $T\Delta S^\ddagger$  values for DSPG flip-flop in bilayers containing 10%, 14.3%, and 25% DSPG have  $T\Delta S^\ddagger$ s of  $105 \pm 10$ ,  $105 \pm 11$ , and  $109 \pm 12$  kJ/mol, respectively, and are statistically identical to pure DSPC ( $101 \pm 26$  kJ/mol). Bilayers composed of 50% and 75% DSPG:DSPC have significantly higher  $T\Delta S^\ddagger$ s for lipid flip-flop of  $127 \pm 12$  and  $127 \pm 16$  kJ/mol, respectively. Figure 5c plots  $T\Delta S^\ddagger$  as a function of bilayer composition to reveal another linear trend that only becomes apparent when considering high concentrations of DSPG. The data in Figure 5 reveal that the amount of DSPG present in the bilayer has a clear effect on the activation energetics for lipid flip-flop; however, the impact is relatively small given the large change in PG concentration examined. One consideration which has not been explored is the charge of the lipid headgroup.

**Charge Screening in DSPG + DSPC Bilayers.** Anionic lipids possess a negative headgroup charge. How this charge

affects the rates and energetics of lipid translocation has not been investigated for PG. The experiments described here were performed in high ionic strength PBS at pH 7.2 in order to model biological conditions. Under these conditions, the Debye length ( $\kappa$ ) is approximately 0.79 nm, which is calculated using the expression:

$$\kappa^{-1} = \sqrt{\frac{\epsilon \epsilon_0 k_B T}{2 c^0 z_i^2 e_0^2}} \quad (6)$$

where  $\epsilon$  is the relative dielectric permittivity of the solvent,  $\epsilon_0$  is the permittivity of the vacuum,  $k_B$  is the Boltzmann constant,  $T$  is the temperature,  $c^0$  is the bulk concentration of ions (per m<sup>3</sup>) in solution,  $z$  is the ion charge, and  $e_0$  is the elementary charge.<sup>47</sup>

The structural similarities between DSPG and DSPC make these lipids completely miscible<sup>48–50</sup> such that the PG headgroups will be evenly dispersed throughout the bilayers. Examination of the surface compressibility<sup>51</sup> obtained from the pressure–area isotherms for the DSPG + DSPC bilayers also confirms that the lipids are completely miscible in the concentration range of DSPG examined here (see the Supporting Information). The effective distance between neighboring DSPG lipids was calculated using an approximate mean molecular area of 45 Å<sup>2</sup>/lipid determined from the Langmuir isotherm at the air/water interface at a surface pressure of 30 mN/m. For the lowest concentrations of DSPG examined here, bilayers composed of 10%, 14.3%, and 25% DSPG, the distance between neighboring lipids is larger than the Debye length at 2.4, 2.0, and 1.5 nm, respectively. Conversely, when the distance between PG lipids approaches the Debye length in the 50% and 75% DSPG:DSPC (1.1 and 0.9 nm, respectively), there is a significant increase in the activation energy. The charge repulsion experienced by neighboring PG lipids in these bilayers and the corresponding increase in  $\Delta G^\ddagger$  indicates that there is an increased energetic penalty for flip-flop when a lipid must re-enter a charged leaflet and the charged headgroup–headgroup repulsion is not adequately screened by the supporting electrolyte. This is consistent with the minimal changes in the energetics observed in bilayers containing small fractions of DSPG where the negatively charged headgroups are dispersed enough to experience little to no charge repulsion.

The direct role charge screening plays on DSPG flip-flop can be examined by calculating the electric field profile of the PG headgroup in high ionic strength PBS used in the experiments. This has been done here by treating the PG headgroup as a negative point charge and calculating the spatial decay of the potential according to

$$\frac{\phi}{\phi_0} = e^{-\kappa x} \quad (7)$$

where  $\phi$  is the potential at a distance ( $x$ ) from the point charge (nm),  $\phi_0$  is the initial potential, and  $\kappa$  is the inverse Debye length.<sup>47</sup> The ratio of  $\phi/\phi_0$  as a function of distance is plotted in Figure 6a with the specific PG–PG separations for the various membrane compositions highlighted. Using the values obtained from Figure 6a, a plot of  $\Delta G^\ddagger$  as a function of  $\phi/\phi_0$  calculated at the PG–PG separation distance for each of the DSPC + DSPG mixtures is shown in Figure 6b.

In order to experimentally verify the role of charge screening on modulating the energetics of DSPG flip-flop, the buffer concentration was adjusted such that the DSPG lipids in



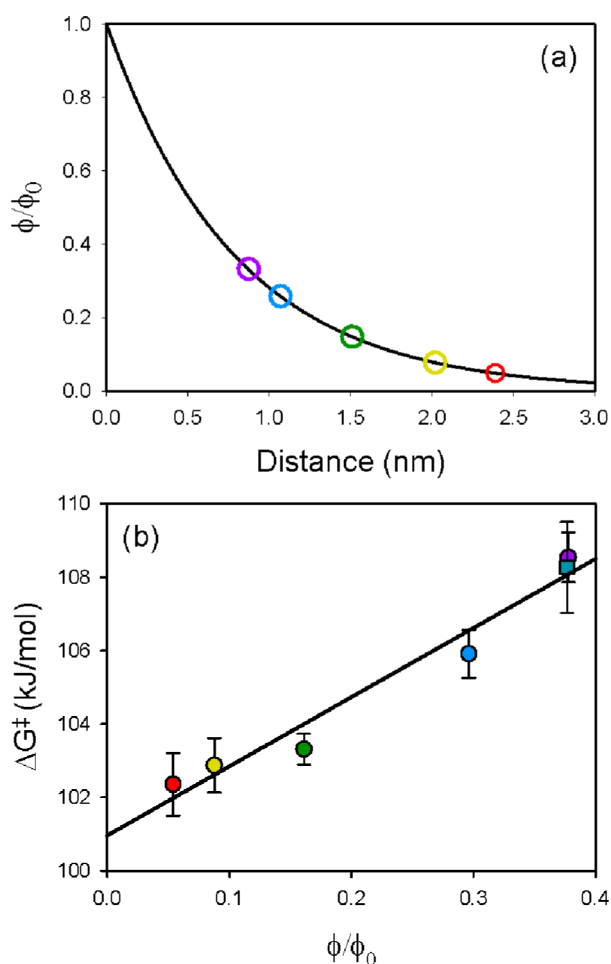


**Figure 6.** (a) Electrostatic potential as a function of distance calculated for the high ionic strength ( $\sim 150$  mM) PBS. The circles represent the PG–PG separations (nm) for membranes containing 10% (red), 14.3% (yellow), 25% (green), 50% (blue), and 75% (purple) DSPG. (b) Activation free energy versus potential for each of the bilayer compositions in part a (solid circles) and the  $\Delta G^\ddagger$  for 25% DSPG in low ionic strength ( $\sim 43$  mM) PBS (square).

bilayers composed of 25% DSPG:DSPC would experience the same charge repulsion as DSPG lipids in 75% DSPG:DSPC bilayers in the high ionic strength PBS. This was done by using eqs 6 and 7 to calculate the electrostatic potential experienced by neighboring PG lipids in the 75% DSPG:DSPC bilayers in the high ionic strength PBS. DSPG in a 25% DSPG:DSPC bilayer placed in a low ionic strength ( $\sim 43$  mM) PBS solution with a calculated Debye length of 1.47 nm, should experience the same potential as a 75% DSPG:DSPC bilayer in the high ionic strength ( $\sim 150$  mM) PBS; see Figure 6a. Under these conditions, similar energetics of lipid flip-flop should be observed in both bilayer compositions if the charge repulsion of PG headgroups is indeed driving the energetics of DSPG flip-flop.

The rate of DSPG flip-flop in bilayers composed of 25% DSPG:DSPC was measured in 43 mM buffer as a function of temperature, and the corresponding  $\Delta G^\ddagger$ s are plotted in Figure 4. The data show that there is extremely good agreement between the energetics of DSPG flip-flop in bilayers composed of 25% DSPG:DSPC and 75% DSPG:DSPC when the buffer strength is adjusted such that neighboring PG lipids experience the same potential in both bilayer compositions. The DSPG

data in 43 mM PBS were fit to eq 5, and the activation energetics for DSPG flip-flop were determined at 40 °C (Table 2). The calculated  $\Delta G^\ddagger$  for DSPG flip-flop at 40 °C in bilayers composed of 25% DSPG in 43 mM PBS was  $108 \pm 1$  kJ/mol. This value is statistically identical to the  $\Delta G^\ddagger$  in bilayers composed of 75% DSPG in 150 mM PBS ( $108.5 \pm 0.7$  kJ/mol). Table 2 reveals that the  $\Delta H^\ddagger$  ( $236 \pm 22$  kJ/mol) and  $T\Delta S^\ddagger$  ( $128 \pm 22$  kJ/mol) for lipid flip-flop in bilayers composed of 25% DSPG in 43 mM PBS are identical to the energetics in bilayers composed of 75% DSPG in 150 mM PBS. The dependence of  $\Delta G^\ddagger$  on potential for 25% DSPG in 43 mM PBS and 75% DSPG in 150 mM PBS also shows excellent agreement, Figure 6b.

The analysis presented above suggests that the energetics of DSPG flip-flop in these mixed DSPG + DSPC bilayers is dictated by charge repulsion between neighboring PG headgroups. Specifically, when DSPG comprises a small portion of the bilayer, the electrostatic potential of neighboring PG lipids are effectively shielded from each other and little to no charge repulsion occurs. Consequently, the energetics of lipid flip-flop in these bilayers are nearly identical, not only to each other, but also to that of pure DSPC lipid flip-flop. Unless the DSPG lipids are close enough to experience charge repulsion from neighboring PG lipids, as in bilayers containing a large fraction of DSPG, or for bilayers in low ionic strength solutions, there is minimal impact of headgroup charge on the energetics of lipid flip-flop.

## CONCLUSIONS

SFVS was used here to quantify the kinetics and thermodynamics of DSPG flip-flop in a range of DSPG + DSPC bilayer compositions. The data presented here show that the activation energetics are directly dependent on the amount of DSPG present in the bilayer. Selective deuteration was used to independently probe lipid flip-flop of the DSPG and DSPC components in these mixed bilayers. The data revealed that the measured activation energies for flip-flop were identical for both lipid components.

When DSPG is present in small quantities in bilayers composed of 10%, 14.3%, and 25% DSPG, only minor changes in the energetics are observed. The significant increase in the  $\Delta G^\ddagger$  and corresponding  $\Delta H^\ddagger$  and  $T\Delta S^\ddagger$  observed in bilayers composed of 50% and 75% DSPG is the result of charge repulsion between PG headgroups. This was experimentally confirmed by altering the buffer conditions such that neighboring PG lipids in bilayers composed of 25% and 75% DSPG experienced the same relative electrostatic potential. The identical  $\Delta G^\ddagger$ s measured for DSPG flip-flop under these conditions confirm that the charge repulsion between neighboring PG headgroups is the driving force behind the energetics of lipid flip-flop in the DSPC + DSPG bilayers examined here. For biological membranes, where the concentration of PG is relatively low, the neighboring PG lipids are spaced far enough apart that their anionic charges are effectively shielded, suggesting that under physiological conditions the charged nature of the headgroup does little to modulate its lipid flip-flop energetics and corresponding rate of translocation.

## ASSOCIATED CONTENT

### Supporting Information

The Supporting Information is available free of charge on the ACS Publications website at DOI: 10.1021/acs.jpcb.5b05523.

Representative pressure–area isotherms of DSPC, DPSG, and the binary DSPG + DSPG mixtures and surface pressure versus surface compressibility curves of the pure and binary lipid mixtures (PDF).

## AUTHOR INFORMATION

### Corresponding Author

\*E-mail: [conboy@chem.utah.edu](mailto:conboy@chem.utah.edu).

### Notes

The authors declare no competing financial interest.

## ACKNOWLEDGMENTS

This work was supported by funds from the National Science Foundation (Grants 1110351 and 1402901).

## REFERENCES

- (1) Dowhan, W. Molecular Basis for Membrane Phospholipid Diversity: Why Are There So Many Lipids? *Annu. Rev. Biochem.* **1997**, *66*, 199–232.
- (2) Devlin, T. M. *Textbook of Biochemistry: With Clinical Correlations*; Wiley-Liss: Hoboken, NJ, USA, 2006.
- (3) Daleke, D. L. Regulation of Transbilayer Plasma Membrane Phospholipid Asymmetry. *J. Lipid Res.* **2003**, *44*, 233–242.
- (4) Pan, J.; Heberle, F. A.; Tristram-Nagle, S.; Szymanski, M.; Koepfinger, M.; Katsaras, J.; Kučerka, N. Molecular Structures of Fluid Phase Phosphatidylglycerol Bilayers as Determined by Small Angle Neutron and X-Ray Scattering. *Biochim. Biophys. Acta, Biomembr.* **2012**, *1818*, 2135–2148.
- (5) Caruso, B.; Mangiarotti, A.; Wilke, N. Stiffness of Lipid Monolayers with Phase Coexistence. *Langmuir* **2013**, *29*, 10807–10816.
- (6) Horvath, S. E.; Daum, G. Lipids of Mitochondria. *Prog. Lipid Res.* **2013**, *52*, 590–614.
- (7) Chen, S.; Liu, D.; Finley, R. L.; Greenberg, M. L. Loss of Mitochondrial DNA in the Yeast Cardiolipin Synthase Crd1 Mutant Leads to up-Regulation of the Protein Kinase Swel1p That Regulates the G2/M Transition. *J. Biol. Chem.* **2010**, *285*, 10397–10407.
- (8) Harwood, J. *Lipids in Plants and Microbes*; Springer: Dordrecht, The Netherlands, 2012.
- (9) Zhang, Y.-P.; Lewis, R. N. A. H.; McElhaney, R. N. Calorimetric and Spectroscopic Studies of the Thermotropic Phase Behavior of the N-Saturated 1,2-Diacylphosphatidylglycerols. *Biophys. J.* **1997**, *72*, 779–793.
- (10) Colbeau, M.; Herve, P.; Fellmann, P.; Devaux, P. F. Transmembrane Diffusion of Fluorescent Phospholipids in Human Erythrocytes. *Chem. Phys. Lipids* **1991**, *57*, 29–37.
- (11) Connor, J.; Schroit, A. J. Transbilayer Movement of Phosphatidylserine in Erythrocytes: Inhibition of Transport and Preferential Labeling of a 31 000-Dalton Protein by Sulfhydryl Reactive Reagents. *Biochemistry* **1988**, *27*, 848–851.
- (12) Daleke, D. L.; Lyles, J. V. Identification and Purification of Aminophospholipid Flippases. *Biochim. Biophys. Acta, Mol. Cell Biol. Lipids* **2000**, *1486*, 108–127.
- (13) Elvington, S. M.; Nichols, J. W. Spontaneous, Interventricular Transfer Rates of Fluorescent, Acyl Chain-Labeled Phosphatidylcholine Analogs. *Biochim. Biophys. Acta, Biomembr.* **2007**, *1768*, 502–508.
- (14) Fellmann, P.; Zachowski, A.; Devaux, P. F. Synthesis and Use of Spin-Labeled Lipids for Studies of the Transmembrane Movement of Phospholipids. *Methods Mol. Biol.* **1994**, *27*, 161–175.
- (15) Haest, C. W. M. Distribution and Movement of Membrane Lipids. In *Red Cell Membrane Transport in Health and Disease*; Bernhardt, I., Ellory, J. C., Eds.; Springer-Verlag: Berlin, Germany, 2003; pp 1–25.
- (16) Henderson, T. O.; Glonek, T.; Myers, T. C. Phosphorus-31 Nuclear Magnetic Resonance Spectroscopy of Phospholipids. *Biochemistry* **1974**, *13*, 623–628.
- (17) Homan, R.; Pownall, H. J. Transbilayer Diffusion of Phospholipids: Dependence on Headgroup Structure and Acyl Chain Length. *Biochim. Biophys. Acta, Biomembr.* **1988**, *938*, 155–166.
- (18) Hrafnisdottir, S.; Nichols, J. W.; Menon, A. K. Transbilayer Movement of Fluorescent Phospholipids in Bacillus Megaterium Membrane Vesicles. *Biochemistry* **1997**, *36*, 4969–4978.
- (19) Khalifat, N.; Rahimi, M.; Bitbol, A.-F.; Seigneuret, M.; Fournier, J.-B.; Puff, N.; Arroyo, M.; Angelova, M. I. Interplay of Packing and Flip-Flop in Local Bilayer Deformation. How Phosphatidylglycerol Could Rescue Mitochondrial Function in a Cardiolipin-Deficient Yeast Mutant. *Biophys. J.* **2014**, *107*, 879–890.
- (20) McConnell, H. M.; Kornberg, R. D. Inside-Outside Transitions of Phospholipids in Vesicle Membranes. *Biochemistry* **1971**, *10*, 1111–1120.
- (21) Martin, O. C.; Pagano, R. E. Transbilayer Movement of Fluorescent Analogs of Phosphatidylserine and Phosphatidylethanolamine at the Plasma Membrane of Cultured Cells. Evidence for a Protein-Mediated and ATP-Dependent Process(es). *J. Biol. Chem.* **1987**, *262*, 5890–5898.
- (22) Pownall, H. J.; Smith, L. C. Pyrene-Labeled Lipids: Versatile Probes of Membrane Dynamics in Vitro and in Living Cells. *Chem. Phys. Lipids* **1989**, *50*, 191–211.
- (23) Zhelev, D. V. Exchange of Monooleoylphosphatidylcholine with Single Egg Phosphatidylcholine Vesicle Membranes. *Biophys. J.* **1996**, *71*, 257–273.
- (24) Kiessling, V.; Crane, J. M.; Tamm, L. K. Transbilayer Effects of Raft-Like Lipid Domains in Asymmetric Planar Bilayers Measured by Single Molecule Tracking. *Biophys. J.* **2006**, *91*, 3313–3326.
- (25) Nishizuka, Y. Intracellular Signaling by Hydrolysis of Phospholipids and Activation of Protein Kinase C. *Science* **1992**, *258*, 607–614.
- (26) Balasubramanian, K.; Schroit, A. J. Aminophospholipid Asymmetry: A Matter of Life and Death. *Annu. Rev. Physiol.* **2003**, *65*, 701–734.
- (27) Liu, J.; Conboy, J. C. 1,2-Diacyl-Phosphatidylcholine Flip-Flop Measured Directly by Sum-Frequency Vibrational Spectroscopy. *Biophys. J.* **2005**, *89*, 2522–2532.
- (28) Nakano, M.; Fukuda, M.; Kudo, T.; Endo, H.; Handa, T. Determination of Interbilayer and Transbilayer Lipid Transfers by Time-Resolved Small-Angle Neutron Scattering. *Phys. Rev. Lett.* **2007**, *98*, 238101.
- (29) Papadopoulos, A.; Vehring, S.; Lopez-Montero, I.; Kutschenko, L.; Stöckl, M.; Stoeckl, M.; Devaux, P. F.; Kozlov, M.; Pomorski, T.; Herrmann, A. Flippase Activity Detected with Unlabeled Lipids by Shape Changes of Giant Unilamellar Vesicles. *J. Biol. Chem.* **2007**, *282*, 15559–15568.
- (30) Lin, W.-C.; Blanchette, C. D.; Ratto, T. V.; Longo, M. L. Lipid Asymmetry in DlpC/DspC-Supported Lipid Bilayers: A Combined Afm and Fluorescence Microscopy Study. *Biophys. J.* **2006**, *90*, 228–237.
- (31) Anglin, T. C.; Brown, K. L.; Conboy, J. C. Phospholipid Flip-Flop Modulated by Transmembrane Peptides Walp and Melittin. *J. Struct. Biol.* **2009**, *168*, 37–52.
- (32) Anglin, T. C.; Conboy, J. C. Lateral Pressure Dependence of the Phospholipid Transmembrane Diffusion Rate in Planar-Supported Lipid Bilayers. *Biophys. J.* **2008**, *95*, 186–193.
- (33) Anglin, T. C.; Conboy, J. C. Kinetics and Thermodynamics of Flip-Flop in Binary Phospholipid Membranes Measured by Sum-Frequency Vibrational Spectroscopy. *Biochemistry* **2009**, *48*, 10220–10234.
- (34) Anglin, T. C.; Cooper, M. P.; Li, H.; Chandler, K.; Conboy, J. C. Free Energy and Entropy of Activation for Phospholipid Flip-Flop in Planar Supported Lipid Bilayers. *J. Phys. Chem. B* **2010**, *114*, 1903–1914.
- (35) Anglin, T. C.; Liu, J.; Conboy, J. C. Facile Lipid Flip-Flop in a Phospholipid Bilayer Induced by Gramicidin A Measured by Sum-Frequency Vibrational Spectroscopy. *Biophys. J.* **2007**, *92*, L01–L03.
- (36) Brown, K. L.; Conboy, J. C. Electrostatic Induction of Lipid Asymmetry. *J. Am. Chem. Soc.* **2011**, *133*, 8794–8797.



- (37) Brown, K. L.; Conboy, J. C. Lipid Flip-Flop in Binary Membranes Composed of Phosphatidylserine and Phosphatidylcholine. *J. Phys. Chem. B* **2013**, *117*, 15041–15050.
- (38) Liu, J.; Brown, K. L.; Conboy, J. C. The Effect of Cholesterol on the Intrinsic Rate of Lipid Flip-Flop as Measured by Sum-Frequency Vibrational Spectroscopy. *Faraday Discuss.* **2013**, *161*, 45–61.
- (39) Liu, J.; Conboy, J. C. Direct Measurement of the Transbilayer Movement of Phospholipids by Sum-Frequency Vibrational Spectroscopy. *J. Am. Chem. Soc.* **2004**, *126*, 8376–8377.
- (40) Wu, F.-G.; Yang, P.; Zhang, C.; Han, X.; Song, M.; Chen, Z. Investigation of Drug-Model Cell Membrane Interactions Using Sum Frequency Generation Vibrational Spectroscopy: A Case Study of Chlorpromazine. *J. Phys. Chem. C* **2014**, *118*, 17538–17548.
- (41) Wu, F.-G.; Yang, P.; Zhang, C.; Li, B.; Han, X.; Song, M.; Chen, Z. Molecular Interactions between Amantadine and Model Cell Membranes. *Langmuir* **2014**, *30*, 8491–8499.
- (42) Zhang, C.; Wu, F.-G.; Hu, P.; Chen, Z. Interaction of Polyethylenimine with Model Cell Membranes Studied by Linear and Nonlinear Spectroscopic Techniques. *J. Phys. Chem. C* **2014**, *118*, 12195–12205.
- (43) Liu, J.; Conboy, J. C. Structure of a Gel Phase Lipid Bilayer Prepared by the Langmuir-Blodgett/Langmuir-Schaefer Method Characterized by Sum-Frequency Vibrational Spectroscopy. *Langmuir* **2005**, *21*, 9091–9097.
- (44) Steinfeld, J. I.; Francisco, J. S.; Hase, W. L. *Chemical Kinetics and Dynamics*, 2nd ed.; Prentice-Hall: Englewood, NJ, USA, 1998.
- (45) Houston, P. L. *Chemical Kinetics and Reaction Dynamics*; Dover: Mineola, NY, USA, 2001.
- (46) Sapay, N.; Bennett, W. F. D.; Tieleman, D. P. Molecular Simulations of Lipid Flip-Flop in the Presence of Model Transmembrane Helices. *Biochemistry* **2010**, *49*, 7665–7673.
- (47) Bard, A. J.; Faulkner, L. R. *Electrochemical Methods: Fundamentals and Applications*, 2nd ed.; John Wiley & Sons: New York, 2001.
- (48) El Mashak, E. M.; Lakhdar-Ghazal, F.; Tocanne, J. F. Effect of pH, Mono- and Divalent Cations on the Mixing of Phosphatidylglycerol with Phosphatidylcholine. A Monolayer ( $\Pi$ ,  $\Delta V$ ) and Fluorescence Study. *Biochim. Biophys. Acta, Biomembr.* **1982**, *688*, 465–474.
- (49) Garidel, P.; Johann, C.; Mennicke, L.; Blume, A. The Mixing Behavior of Pseudobinary Phosphatidylcholine-Phosphatidylglycerol Mixtures as a Function of  $\Phi$  and Chain Length. *Eur. Biophys. J.* **1997**, *26*, 447–459.
- (50) *Thermotropic Phase Transitions of Pure Lipids in Model Membranes and Their Modifications by Membrane Proteins*; Silvius, D. J. R., Ed.; John Wiley & Sons: New York, 1982.
- (51) Lozano, M. M.; Longo, M. L. Complex Formation and Other Phase Transformations Mapped in Saturated Phosphatidylcholine/DsPE-Peg2000 Monolayers. *Soft Matter* **2009**, *5*, 1822–1834.